Supporting Information

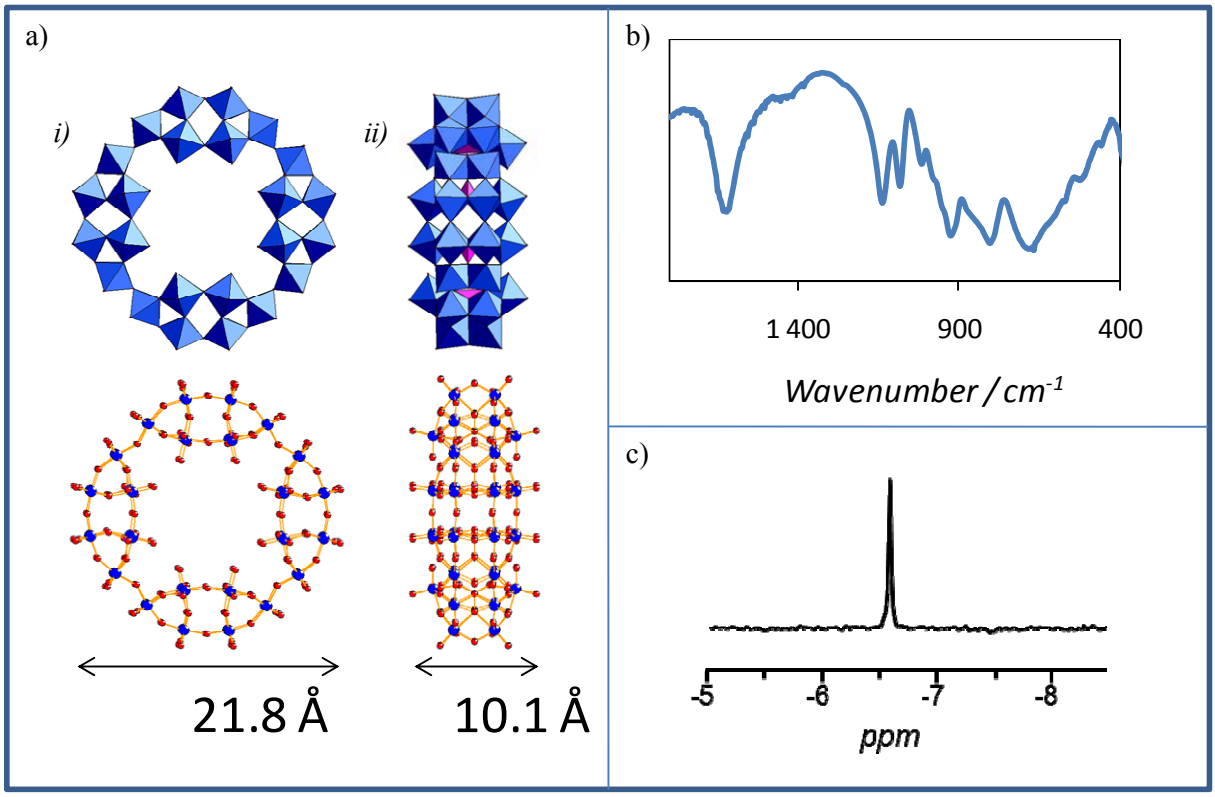

Figure 1. (a) Face and side views of the superlacunary POM $[H_7P_8W_{48}O_{184}]^{33-}$ in polyhedral representation (top) and in ball-and-stick representation (down). In the first representation, the WO_6 octahedra are depicted in blue, whereas the PO_4 tetrahedra are represented in pink. In the latter, phosphorus atoms are depicted in pink, tungsten atoms in blue and oxygen atoms in red. The $[H_7P_8W_{48}O_{184}]^{33-}$ part is represented by red and yellow polyhedra. **(b)** FT-IR spectrum of P_8W_{48} in KBr pellet. Wavenumbers in cm^{-1}: 1625 (s), 1140 (s), 1085 (s), 1017 (m), 927 (vs), 805 (vs), 684 (vs). **(c)** ^{31}P NMR spectrum of P_8W_{48} in D_2O/H_2O.

Supporting Information

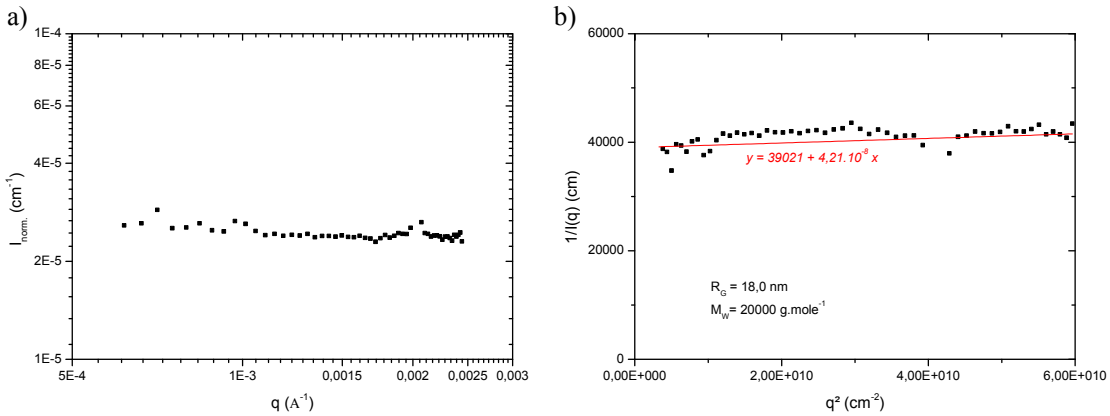

Figure 2. (a)Variation of the scattered intensity, I, with q over the following ranges: $6.8 \times 10^{-4} \leq q$ ($Å^{-1}$) $\leq 2.4 \times 10^{-3}$ (Static light scattering) for dilute aqueous gelatin solution (c = 0.1 wt.%) at 50 °C, I = 0.1 M and pH = 3.4. (b) Representation of the same data than above but 1/I(q) vs q².

Supporting Information

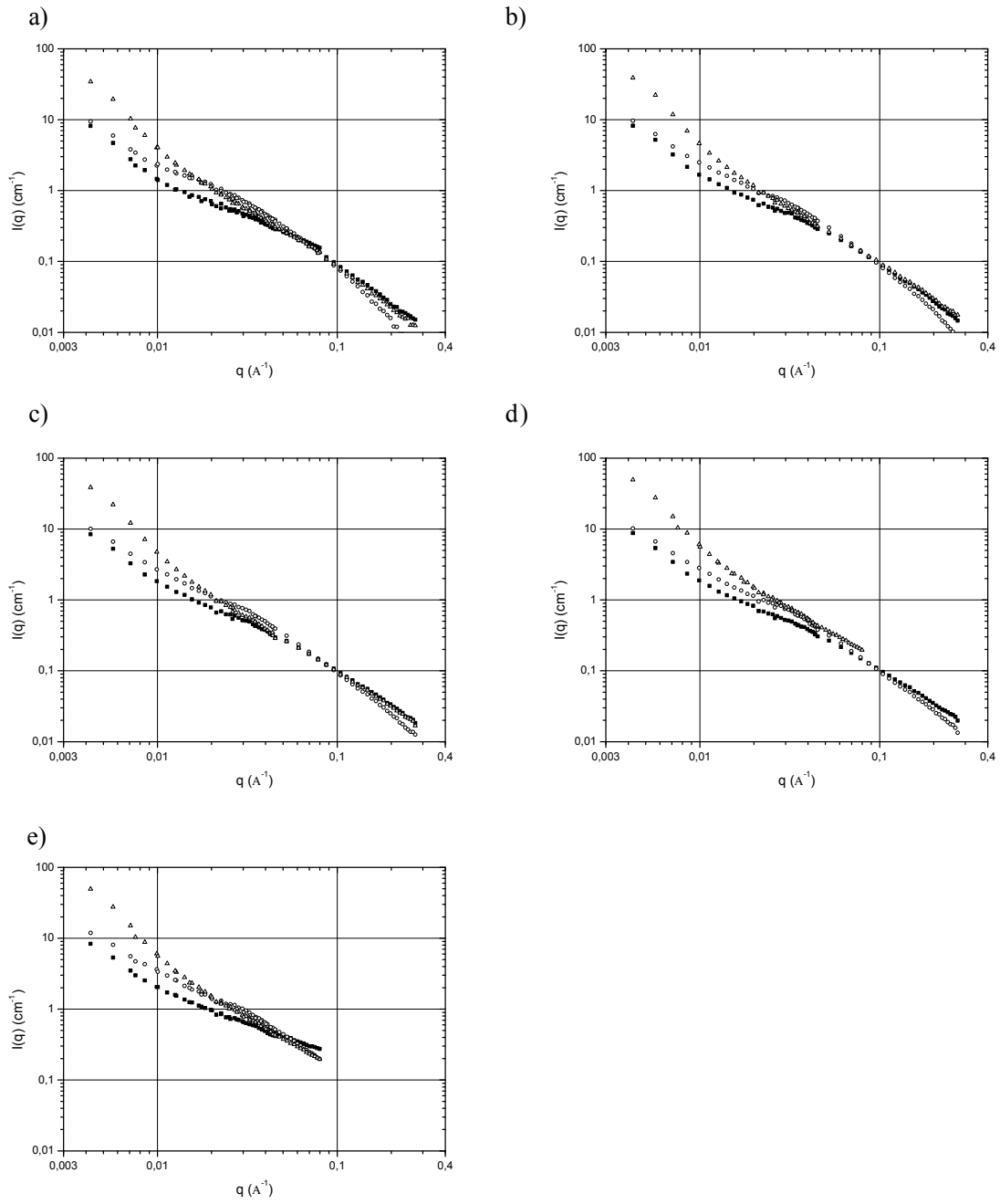

Figure 3. Variation of the scattered intensity, I, with q in pure D_2O solvent for the reference gelatin sample ([gelatin] = 10 wt.%, full square) and for the nanocomposite samples: $[H_7P_8W_{48}O_{184}]^{33-}$ = 0.37 wt.% / [gelatin] = 10 wt.% (blank circle) and $[SiO_2]$ = 0.2 wt.% / [gelatin] = 10 wt.% (blank triangle) at different times: (a) t_0, (b) t_1, (c) t_2, (d) t_3, (e) t_4. The corresponding helix amounts are summarized in table 2 for the 3 systems.

Supporting Information

Complement to Materials and Methods

1. Thermal protocol for "sol-gel" transition.

For SANS and polarimetry measurements the samples were submitted to the same thermal protocol (see S.I.). (1) T = 50°C during 5h; (2) Cooling at 0.5°C.min^{-1} to 27 °C; (3) T = 27 °C during 15 h; (4) Cooling at 0.5°C.min^{-1} to 11 °C; (5) T = 11 °C during 50 h; (6) Heating at 0.5°C.min^{-1} to 50 °C and (7) T = 50°C during 5h. SANS measurements were performed at t_0 = 30 min (step 1 : T = 50 °C), t_1 = 6 h 40 min (step 3 : T = 27 °C), t_2 = 10 h 50 min (step 3 : T = 27 °C), t_3 = 15 h 00 min (step 3 : T = 27 °C), t_4 = 24 h 30 min (step 5 : T = 11 °C), t_5 = 65 h 30 min (step 5 : T = 11 °C) and t_6 = 72 h 30 min (step 7 : T = 50 °C). These times determine the beginning of the measurements that run for 1h30 in the intermediate configuration.

2. Static and Dynamic Light scattering

Static Light Scattering (SLS) and Dynamic Light Scattering (DLS) measurements were performed using a 3D DLS spectrometer (LS Instruments, Fribourg, Switzerland) equipped with a 25mW HeNe laser (JDS uniphase) operating at λ=632.8 nm, a two channel multiple tau correlator (1088 channels in autocorrelation), a variable-angle detection system, and a temperature-controlled index matching vat (LS Instruments). The scattering spectrum was measured using two single mode fibre detections and two high sensitivity APD detectors (Perkin Elmer, model SPCM-AQR-13-FC). Solutions were directly filtered through a 0.2 µm cellulose millipore filter into the cylindrical scattering cells and temperature was fixed at 25.0 ± 0.1 °C or 50.0 ± 0.1 °C depending on the experiments.

In the SLS experiments, the excess of scattered intensity $I(q)$ was measured with respect to the solvent, where the magnitude of the scattering wave vector q is given by

$$q = (4\pi n/\lambda)\sin(\theta/2) \qquad (1)$$

where n is the refractive index of the solvent (1.34 for water at 25 °C), and θ is the scattering angle. In our experiments, θ was varied between 30 ° and 130 °, which corresponds to scattering wave vectors, q, in the range from 6.8×10^{-3} to 2.4×10^{-2} nm^{-1}.

The absolute scattering intensities I (in cm^{-1}) (i.e., the excess Rayleigh ratio) were deduced by using a toluene sample reference for which the Rayleigh ratio is well-known (14×10^{-6} cm^{-1} at 633 nm). A virial expression for the osmotic pressure can be used in dilute regime to deduce the following relationship:

$$\frac{Kc}{I(q,c)} = \frac{1}{M_W}\left[1 + q^2\frac{R_G^2}{3} + \cdots\right] + 2A_2Q(q,c)c + \cdots \quad (2)$$

The function $Q(q,c)$ is approximately unity for flexible polymer chains, but not for spheres;[31] $Q(0,c)$ is equal to 1 in any case. c is the polymer concentration, and A_2 is the second virial coefficient, which describes the polymer-solvent interactions. The scattering constant is $K = 4\pi^2n^2(dn/dc)^2/N_A\lambda^4$, where dn/dc is the refractive index increment and N_A is Avogadro's number. The dn/dc of gelatin [32] and silica nanoparticle[33] in 0.1 M NaCl aqueous solutions is equal to 0.18 and 0.074 cm^3.g^{-1}, respectively. The plots of $c/I(q,c)$ *versus* q^2 were extrapolated to $q = 0$ to give intercepts $c/I(0,c)$. If the length scale q^{-1} is sufficiently large compared to the radius of gyration R_G of the polymers, the form factor obeys Guinier's law, and the apparent radius of gyration $R_{G,app}$ can be determined from the intercept and the initial slope of these plots using a scattering inverse Lorentzian law of the form[31]

$$\frac{c}{I(q,c)} = \frac{c}{I(0,c)}\left[1 + q^2\frac{R_{G,app}^2}{3}\right] \qquad if\ qR_G \ll 1 \qquad (3)$$

The weight-average molecular weight[31] M_w can be obtained from

$$\frac{I(0,c)}{Kc} = M_{W,app} = M_W(1 - 2A_2M_Wc) \qquad (4)$$

The apparent mass $M_{w,app}$ of polymers in solution at a concentration c is given by extrapolation of the scattered intensity $I(q)/c$ to $q = 0$, while the apparent radius of gyration is obtained by a mean-square linear fit of the inverse of the scattered intensity *vs* q^2.

In the dynamic light scattering experiments (DLS), the experimental signal is the normalized time autocorrelation function of the scattered intensity [34,35]

$$g^{(2)}(q,t) = \frac{\langle I(q,0).I(q,t)\rangle}{\langle I(q,0)\rangle^2} \qquad (5)$$

The latter can be expressed in terms of the field autocorrelation function or equivalently in terms of the autocorrelation of the concentration fluctuations, $g^{(1)}(q,t)$ through:

$$g^{(2)}(q,t) - 1 = \alpha + \beta.\left|g^{(1)}(q,t)\right|^2 \qquad (6)$$

where α is the baseline (varying between 1×10^{-4} and 2×10^{-4} in our experiments) and β the coherence factor, which in our experiments is equal to 0.8–0.9. The normalized correlation function, $g^{(1)}(q,t)$, of polymer concentration fluctuation is defined as

$$g^{(1)}(q,t) = \frac{\langle \delta c(q,0).\delta c(q,t)\rangle}{\langle \delta c(q,0)^2\rangle} \qquad (7)$$

where $\delta c(q,t)$ and $\delta c(q,0)$ represent fluctuations of the polymer concentration at time t and 0, respectively.
Dilute solutions of polymer or nanoparticles were characterized by a single relaxation mechanism with a characteristic time inversely proportioned to q^2. For these solutions, we have applied the classical cumulant analysis. This analysis provides the variance of the correlation function and the first reduced cumulant $(\tau q^2)^{-1}$, where τ is the average relaxation time of $g^{(1)}(q,t)$. The extrapolation of $(\tau q^2)^{-1}$ to $q = 0$ yields the values of the diffusion constant D. The latter is related to the average apparent hydrodynamic radius R_H of the diffusing species through the Stokes-Einstein relation

$$D = \frac{k.T}{6.\pi.\eta_S.R_H} = \left(\frac{1}{\tau.q^2}\right)_{q^2=0} \qquad (8)$$

where k is the Boltzmann constant, η_S the solvent viscosity, and T the absolute temperature. The scattering from semi-dilute gelatin solutions was fitted by the sum of two exponentials as discussed in the course of the text.

3. Optical rotation

Gelatin is an optically-active material in both the coil and helical states. Due to coherent chiral ordering helical domains rotate the plane of light polarization much more strongly than the individual chiral amino acids in the coil state. Thus, the coherent optical activity gives a direct indication of the fraction of the monomers in the helical states. Optical rotation was measured on a Perkin-Elmer 341 polarimeter, equipped with a computer collecting simultaneously the optical rotation angle and the temperature of the sample versus time. The glass cell has an optical path of 1 cm. The temperature is regulated by a programmable external circulating bath (Julabo FS18). Cooling ramps of about 0.6 °C/min were applied to fit the cooling conditions used during SANS measurements. Taking into account the slightly colored character of our solutions, the validity of the Drude relation[36] was checked by measuring the specific optical rotation at different wavelengths (λ = 365 nm, 436 nm, 546 nm and 578 nm) before each measurement. The measurements were performed with the same wavelength: λ = 436 nm. The procedure of triple helix fraction determination has been previously described and detailed elsewhere.[18,37] We recall that the helix amount (χ) is defined as the ratio between the number of residues in helical conformation and the total number of residues. χ is derived from the following expression :

$$\chi = \frac{[\alpha]_\lambda^{exp} - [\alpha]_\lambda^{coil}}{[\alpha]_\lambda^{collagen} - [\alpha]_\lambda^{coil}} \qquad (9)$$

Where $[\alpha]_\lambda^{exp} = \alpha/c.l$ is the specific optical rotation of the gelatin in solution, c is the concentration (in g.cm^{-3}), l is the optical path (dm), α is the optical rotation angle (degrees) measured experimentally, $[\alpha]_\lambda^{collagen}$ is the specific optical rotation of native soluble collagen (χ = 1), which contains only triple helices, and $[\alpha]_\lambda^{coil}$ is the specific optical rotation of the coils (χ = 0). An average value of 100 g.mol^{-1} per amino acid was considered. At high temperature, it can be assumed that all the chains are in a random coil conformation. The specific optical rotations for the different gelatins in coil conformation were derived directly from the measurement in solutions at high temperature. The helix amounts plotted in figures 12 and 13 correspond to averaged value on 1 h 30 min to take into account the delay of SANS data acquisition.

4. Small angle neutron scattering (SANS)

SANS experiments were carried out on the PACE spectrometer in Léon Brillouin Laboratory at Saclay (LLB, France). The chosen incident wavelength, λ, depends on the set of experiments, as follows. For a given wavelength, the range of the amplitude of the transfer wavevector q was selected by changing the detector distance, D. Three sets of sample-to-detector distances and wavelengths were chosen [D = 4.7 m, λ = (10 ± 0.5) Å; D = 2.5 m, λ = (10 ± 0.5) Å; D = 1.2 m, λ = (6 ± 0.5) Å] so that the following q-ranges were respectively, available: $4.3 \times 10^{-3} < q$ (Å^{-1}) $< 4.52 \times 10^{-2}$, $7.5 \times 10^{-3} < q$ (Å^{-1}) $< 7.99 \times 10^{-2}$, $2.62 \times 10^{-2} < q$ (Å^{-1}) $< 2.72 \times 10^{-1}$. Measured intensities were calibrated to absolute values (cm^{-1}), using normalization by the attenuated direct beam classical method. Standard procedures to correct the data for the transmission, detector efficiency, and backgrounds (solvent, empty cell, electronic, and neutronic background) were carried out. To combine data from light and neutron scattering it is necessary to rescale the SLS data to give the overlap with the SANS data. The light scattering intensity at each q value was adjusted by the ratio between the contrasts of the two techniques so that the SLS data overlap with the SANS data in the region of comparable q. The scattering profiles cover then a q range of nearly 3 decades. The usual equation for absolute neutron scattering combines the intra-scattering object form factor $S_1(q)=V_{chain}.\phi_{vol}.P(q)$ with the inter-scattering object structure factor $S_2(q)$:

$$I(q) = (\Delta\rho)^2.\big(S_1(q) + S_2(q)\big) \qquad (10)$$

where $(\Delta\rho)^2 = (\rho_{monomer} - \rho_{solvent})^2$ is a contrast per volume unit between the scattering object and the solvent and was determined from the known chemical composition.
$\rho = (\sum_i n_i b_i)/(N_A.\sum_i n_i m_i v)$ represents the scattering length per unit volume, b_i is the neutron scattering length of the species i, m_i the mass of species i, and v the specific volume of the monomer or the solvent (i.e., 0.9 cm^3/g for deuterated water). $P(q)$ is the form factor, $V_{chain} = Nvm \times 1.66 \times 10^{-24}$ is the volume of the N monomers (of mass m) in a chain and ϕ_{vol} is the volume fraction of monomer. In the high q-range, the scattering is assumed to arise from isolated assemblies; i.e., $S_2(q) = 0$, and thus $I(q) \propto P(q)$. Each sample was achieved either in a 100 % D_2O solvent or in a 72%/28% H_2O/D_2O solvent that matches the gelatin contribution-so that the signal is only arising from the inorganic nanoparticles.

5. Small angle X-ray scattering (SAXS)

Small-angle X-ray scattering (SAXS) experiments were performed on the Swing beamline at SOLEIL synchrotron, Saint-Aubin (France). The incident beam energy was 12.0 keV (λ = 1.35 Å), and the distance from the sample to the Aviex CCD detector was 1435.8 mm. The corresponding scattering vector q varied from 0.007 to 0.7 $Å^{-1}$. Experiments were performed at 25 °C. Several successive frames (typically 10) of 1 s each were recorded for both the sample and the solvent (water). We checked that X-rays did not cause any damage to the particles by comparing successive frames. The average intensity and experimental error of each set of frames were subsequently computed. Scattering from the solvent was measured and subtracted from the corresponding intensity of tannin solution. The scattering data were normalized to constant beam intensity and corrected for transmission, sample thickness, parasitic, and background scattering. The resulting scattering profiles are obtained as normalized intensities in relative units versus scattering vector q.